RTAB: the Rayleigh scattering database

Lynn Kissel[†]
V Division, Physics Directorate
Lawrence Livermore National Laboratory
Livermore, CA 94551-0808
USA

UCRL-JC-137026
Revised August 8, 2000

Abstract

Systematic tabulations of differential scattering cross sections for all atoms for photon energies 0.0543-2754.1 keV in various approximations are being made available, with a focus on the S-matrix approach of Kissel and Pratt. New tabulations are also being made available of: anomalous scattering factors for 0-10 MeV; total-atom, shell and subshell form factors; bound-bound oscillator strengths; total-atom, shell and subshell photoeffect cross sections; and Dirac-Slater potentials. Accurate interpolation of S-matrix cross sections to intermediate energies is investigated. Selected computer codes that generate or use these data are described.

1. Introduction

Our knowledge about elastic photon-atom scattering has been significantly advanced by research efforts originating from, or coordinated with Richard Pratt and co-workers from the University of Pittsburgh.[1] All these investigations, spanning more than three decades, had Richard Pratt as a primary motivating influence. This author's 25-year involvement with these studies simply could not have been sustained without Richard Pratt's support.

Although the results of numerous scattering studies have been published, only a small fraction of the actual scattering data have been made available in the form of traditional print. Aside from the issue of volume, traditional print distribution does not readily satisfy the reuse of this information in computer calculations. Therefore, an electronic form for distribution for our scattering data is desirable. A subset of our data has been available for some time on the Internet from a World-Wide-Web site at Lawrence Livermore National Laboratory, accessible through the URL (uniform resource locator)

http://www-phys.llnl.gov/Research/scattering/

This report describes a new expanded database of scattering-related information. In addition to its availability on the Internet, it has also been formatted and recorded to CD-ROM (compact disc, read-only-memory). This medium has some advantages for distribution to areas without reliable high-speed access to the Internet. It is also a more static medium than the World Wide Web.

[†] Current address: Scientific Computing and Communications Department, Lawrence Livermore National Laboratory, Livermore, CA 94551-0808, USA

[1] A list of reports prepared by Richard Pratt's research group at the University of Pittsburgh contains over 110 manuscripts dealing primarily with photon scattering. Well over half of these have been published in refereed scientific journals or conference proceedings.

2. Calculating Rayleigh amplitudes and cross sections

Considerable progress has been made in the last half of the twentieth century in the practical evaluation of elastic photon scattering by atoms. Three main avenues of increasing computational complexity have emerged to yield practical predictions: the form factor approximation, anomalous scattering factors for forward-angle scattering, and predictions based on the second-order S-matrix element. For an assessment of the validity of simpler approaches to scattering see Kissel et al. (1995); for a review of elastic scattering focused on the low-energy ã-ray region see Kane et al. (1986).

The form factor approximation, valid for photon energies much greater than electron binding energies and for non-relativistic momentum transfers, has been extensively tabulated. Tables of nonrelativistic form factors (Hubbell et al., 1975), relativistic form factors (Hubbell and Øverbø, 1979) and modified relativistic form factors (Schaupp et al., 1983) for all neutral atoms have been published.

Anomalous scattering factors are a forward-angle energy-dependent result computed via the dispersion relation and optical theorem. Predictions are now readily available for all atoms for keV energies due to a work pioneered by Cromer and Liberman (Cromer and Liberman, 1970a,b, 1976, 1981; Cromer, 1974, 1983; Creagh and McAuley, 1992; Henke et al., 1981, 1993). Anomalous scattering factors have been used in conjunction with form factors to yield corrected differential scattering predictions.

Numerical evaluation of the S-matrix element is a more sophisticated approach to the evaluation of elastic photon scattering by atoms. Contained within this approximation is the high-energy form factor result, as well as the forward-angle energy-dependent anomalous-scattering-factor result. It goes beyond both these approximations to yield predictions valid at all scattering angles and energies. Computationally, it is the most complex of the schemes discussed here, requiring considerable computer time. Due to the dramatic increase in the availability of computers, systematic evaluation of the S-matrix element has now become practical.

Numerical evaluation of the second-order S matrix for single-electron transitions in a potential was first attempted in the 1950's by Brown and co-workers (see, for example, Brown et al., 1955). Further refinements in the technique were introduced by Johnson and co-workers in the 1960's (see, for example, Johnson and Feiock, 1968; Johnson and Cheng, 1976). Kissel, Pratt and co-workers have made extensive studies of the scattering process, focused on predictions utilizing the S-matrix approach (see, for example, Kissel and Pratt, 1985; Kane et al., 1986; Pratt et al., 1994; Kissel et al., 1995). Kissel and Pratt have developed a prescription for practical and accurate predictions of elastic scattering that utilizes S-matrix amplitudes for the contribution from inner-shell electrons ($\hbar\omega \leq 300$å, å is electron binding energy), and modified relativistic form factors to estimate the contribution from outer-shell electrons. This effort has resulted in availability of systematic S-matrix scattering predictions for all atoms, all angles and photon energies from 0.0543-2754 keV.

For x-ray and low-energy ã-ray energies, it is customary to compute the total elastic photon-atom scattering amplitude as the sum of separate amplitudes:

- R – the Rayleigh amplitude, for scattering from the atomic electrons;
- NT – the nuclear Thomson amplitude, for scattering from the nucleus modeled as a point charge;
- D – the Delbrûck amplitude, for scattering from the field of the nucleus;
- NR – and the nuclear resonance amplitude, for scattering from the internal structure of the nucleus modeled by the giant dipole resonance.

For the x-ray and low-energy ã-ray energies considered here, the Rayleigh amplitude dominates the total scattering amplitude for most energies and angles. The nuclear Thomson amplitude is important in the 100-keV range and higher for heavy atoms at intermediate and back angles. Except for heavy atoms and photon energies above about 1 MeV, the Delbrûck and nuclear-resonance amplitudes are not expected to contribute significantly to the total scattering amplitude.

3. Directory structure of the RTAB database

Extensive numerical calculations over the last 25 years by Kissel and Pratt have yielded a systematic self-consistent collection of values. In addition to the S-matrix values themselves, this effort has generated systematic tabulations of related quantities that are of interest for scattering and other investigations. These quantities include self-consistent atomic potentials, form factors, anomalous scattering factors, and bound-bound oscillator strengths. These values and selected programs have been collected in the form of a database that we call RTAB. The directory structure of version 2.0 of the RTAB database is displayed in Table 1.

These values are currently available on-line from the Internet at the following URL

http://www-phys.llnl.gov/Research/scattering/RTAB.html

Table 1

and via FTP (file transport protocol) at

ftp://www-phys.llnl.gov/pub/rayleigh/RTAB

This database has also been recorded onto CD-ROMs and is available from the author. The database is contained on two standard 650-MB CD-ROM discs that are written in an ISO-9660 format, an international standard that specifies how data is formatted on the CD-ROM. ISO 9660 also includes a specification for directory and file names. A CD-ROM written to the ISO 9660 standard can be read on various computer operating systems including DOS, Macintosh, OS/2, Windows and UNIX.

4. UFO library-structured files and (x,y) data tables

Many of the files in the RTAB database utilize a simple library-structured file format. With this format, multiple logical files (or blocks of information) can be tightly associated in a single physical file. The start of a logical file within a UFO-structured library file (Kissel et al., 1991a,b) is designated by a record of the form

*BLOCK:*identifier*

where the asterisk ('*') starts in the first column and '*identifier*' is a string of characters used as a unique identifier for the block of information that follows.

For example, the specification 'data_SCF/047_scf0sl' indicates a file named '047_scf0sl' within the folder (directory) 'data_SCF' in the RTAB database. This file contains the Dirac-Slater self-consistent potential for neutral Silver (Ag, Z=47). Within this physical file is contained the following logical files

*BLOCK:PARAMETERS
*BLOCK:SUMMARY
*BLOCK:CONFIG
*BLOCK:V

This file structure makes it relatively simple for a program (or a human) to locate specific information within the file, and it is used extensively by the elastic scattering codes.

The UFO-specification also defines a mechanism for explicitly referring to these blocks of information by means of extensions to the normal filename, and utility subprograms within the RAYLIB support library implement this capability. For example, a user might specify

047_scf0sl|module=V

as the filename for an elastic-scattering program requiring access to the self-consistent potential for Ag. The vertical bar ("|") is used to separate UFO extensions from the normal filename. In some situations, it may be necessary for the filename to be enclosed in quotes, or for the vertical bar to be "escaped" (e.g., "\|" on Unix systems), to avoid misinterpretation by the computer.

Keywords in UFO extensions can be abbreviated, and multiple non-conflicting extensions can be specified with a single filename. The reference to the potential for Ag above could be abbreviated to

047_scf0sl|m=V

Utility subprograms within the RAYLIB support library allow for the flexible reading of (x,y) data tables prepared in the UFO data format. In addition to simple tables of (x,y) data pairs, more complicated data tables are supported where, for example, the specific columns of a larger table can be selected as the x- and y-data (the independent and dependent variables, respectively), or the data can be transformed after being read from the file.

Specific examples of UFO extensions that will be encountered by a user of the FFTAB code (discussed subsequently) include:

013_mf0sl|m=TOTAL ,

specifies the total-atom modified relativistic form factor for Aluminum (Al, Z=13), selected from a library-structured file that contains separate modules for the total atom ("|m=TOTAL"), individual shell ("|m=K", "|m=L", etc.) and individual subshell ("|m=L1", "|m=L2", etc.) form factors;

006_asf0sl|m=RE|y=3 ,

specifies the real anomalous scattering factor f ' for Carbon (C, Z=6) for use with the relativistic form factor (as opposed to g ' for use with the modified relativistic form factor) from a library file that separately tabulates the real ("|m=RE") and imaginary ("|m=IM") parts, selecting column 3 ("|y=3") for the y values (by default, "|x=1" and "|y=2" – in this example, "|y=2" would select g ');

082_nf0h75|t=0.01220*y ,

computes the non-relativistic form factor *per electron* for Lead (Pb, Z=82) by scaling the existing values in the file by 1/Z ("|t=0.01220*y" specifies a transform whereby the y values read from the file are multiplied by the factor 0.01220 before the values are returned to the calling program[2]).

Many more transformations and extensions are implemented, and the interested reader should consult the UFO documentation for details (Kissel et al., 1991a,b).

5. Dirac-Slater atomic potentials (data_SCF)

The starting point of all our numerical calculations is the model of relativistic single-electron transitions in a local, central potential. We have utilized a modified version of the relativistic Dirac-Slater HEX code (Liberman et al., 1971) to evaluate our atomic potentials. Although HEX was used as the basis for these SCF calculations, initiated over 25 years ago, a fresh start today would utilize a more modern code such as DAVID (Liberman and Zangwill, 1984). A copy of the source for RSCF is included in the code folder of the RTAB database for those who wish to duplicate or extend our work.

[2] The nonrelativistic form factors of Hubbell et al. (1975) are stored in their original form wherein *f(0)=N*, where *N* is the number of electrons in the atom. The FFTAB code needs the form factor per electron (the default form of the modified relativistic form factor, g, and relativistic form factor, f, computed by Kissel).

An important characteristic of the all *our* (as opposed to the work of other authors) elastic scattering data in the RTAB database is that it is consistently computed in the same Dirac-Slater potential. That is, form factors, anomalous scattering factors, photoeffect cross sections, bound-bound oscillator strengths, and S-matrix elements are all computed starting from the same Dirac-Slater potential. As a consequence, comparisons of predictions in different approximations are not unnecessarily complicated by differences in the underlying atomic model. As shown in Figure 1, there is considerable resonance structure in our evaluation of elastic scattering. As a consequence of using the same potential for computing the S-matrix and anomalous-scattering-factor approximations, the resonances shown in Figure 1 occur at exactly the same energy in both approximations. This useful feature will be exploited when we subsequently discuss interpolating on the S-matrix values.

Figure 1

The exceptions to this use of a single underlying potential model is the work of *other* authors (redistributed with their permission) that we've included in the RTAB database for completeness and convenience of potential users. The non-relativistic form factors due to Hubbell et al. (1975) (in 'data_NF'), and the differential scattering cross sections computed from these form factors (in 'tables_NF'), do not result from our Dirac-Slater potential. Also, the anomalous-scattering-factor code and database of Cromer and Liberman (in 'other/CromerLiberman83'; Cromer, 1983), and Henke et al. (1993) (in 'other/Henke93') do not result from our potential. The photoeffect cross sections of Scofield (1973) (in 'other/Scofield73') were computed in a Dirac-Slater potential, although not identically the one provided in the RTAB database.

The potential files are contained in a folder named 'data_SCF' and have filenames of the form 'ZZZ_scfIM' where

ZZZ is a 3 digit integer indicating the atomic number
'_scf' indicates that the file contains self-consistent-potential data,
'I' is an integer indicating the ioniticity ('0' => neutral atom),
'M' is a string indicating details of the atomic model used, some examples are,
'sl' => Slater exchange coefficient with Latter tail (potential goes to as 1/r at large distances),
'kl' => Kohn-Sham exchange coefficient (2/3 the Slater value) with Latter tail,
'cK' => Coulomb potential, electron in K shell.

For example, '082_scf0sl' indicates the potential for neutral Lead (Pb, Z=82) with a Slater-exchange coefficient and Latter-tail approximation.

The Dirac-Slater potentials are stored as UFO library-structured files containing four logical files: 'PARAMETERS' contains the input parameters to the RSCF code used to generate this file; 'SUMMARY' contains a summary report on the results of the calculation; 'CONFIG' contains a report on the electronic configuration of the atom used in the calculation; and 'V' contains the potential as [*r,V(r),Q(r)*] tuples,

6. Differential elastic-scattering cross-section tables (tables_SM, tables_MFASF, tables_RFASF, tables_MF, tables_RF, tables_NF)

The primary goal for preparing the RTAB database was to make extensive tabulations of the differential elastic scattering cross sections and amplitudes readily available. These folders, containing differential cross section tabulations in the following approximations (see, for example, Kissel et al., 1995), are available in the RTAB database:

- **tables_SM** – numerical S-matrix predictions for inner electrons and modified relativistic form-factor predictions for outer electrons due to Kissel and Pratt (our best predictions – most computationally intensive to produce, limitations as noted below);
- **tables _MFASF** – modified relativistic form factors with angle-independent anomalous scattering factors (yields predictions close to SM values in many cases, except for back angles at high energies of heavy atoms – much less computationally intensive to produce than SM

values – predictions for all Z, E, è can be easily prepared using the FFTAB code and data in RTAB database – can be easily extended to ions, excited and hollow atoms, inclusion of experimental information such as more realistic photoeffect thresholds, inclusion of environmental effects such as scattering in plasmas or solids);

- **tables _RFASF** – relativistic form factors with angle-independent anomalous scattering factors (yields predictions identical to MFASF in the forward direction, much poorer predictions for non-forward angles of heavy atoms, especially at 100 keV and higher energies);
- **tables _MF** – modified relativistic form factors (generally the best of the form-factor-only predictions);
- **tables _RF** – relativistic form factors (generally yields poorer predictions than those from the modified relativistic form factor, only);
- **tables _NF** – non-relativistic form factors (Hubbell et al., 1975) (generally yields predictions better than those from relativistic form factors, only).

The numerical S-matrix values are our best predictions, but they have limitations.

- We compute scattering for zero-temperature isolated atoms, neglecting all atomic-environment effects. Interference of the scattering of photons from neighboring atoms is known to make important modifications to photoabsorption near to photoionization thresholds, and thermal diffuse scattering will be important at small momentum transfers. Atom-environment effects in scattering have been observed for solids (see, for example, Gonçalves et al., 1993) and amorphous materials (see, for example, Gonçalves et al., 1994).

- We compute scattering for single-particle transitions in a local potential. This approach only includes a local-density approximation to exchange, neglects correlations, and yields photoionization thresholds that differ noticeably from experiment. Energy scaling procedures have been found to improve predictions near thresholds (Basavaraju et al., 1995) although a more general approach to incorporate experimental information (such as accurate threshold values) is needed. Non-local exchange effects were found to be responsible for the disagreement between our S-matrix predictions and experiment for scattering from Neon (Jung et al., 1998).

  Recent studies (Carney et al., 2000a; Carney and Pratt, 2000) suggest that the neglect of correlations might be partially remedied. Correlations are found to matter most for dipole transitions at low energy, where the anomalous scattering approach is valid. This implies that the S-matrix amplitudes might be replaced by better MFASF predictions, using photoeffect cross sections that include correlations.

- Our prescription utilizes modified form-factor approximation to estimate the contribution for outer electrons (defined in this case as electrons wherein ħù > 300å, å is electron binding energy). We expect that this will be a good approximation for nonrelativistic momentum transfers (ħq << mc), which for back-angle scattering translates to ħù << ½mc^2. At large momentum transfers, *s*-states dominate the scattering amplitude with a contribution related to the square of the wavefunction normalization. As a consequence, inner-shell *s*-states strongly dominate over outer-shells.

  For intermediate and back angles for photon energies greater than about 100 keV, we expect that our MF approximation will be an increasingly poor estimate for the scattering from outer electrons. Under our definition, *all* electrons for Carbon ($å_K$ ~ 300 eV), as an example, are estimated by MF by about 100 keV. In general it is anticipated that the Rayleigh scattering amplitude is very small under these circumstances, and the errors introduced by use of MF are likely masked by the contribution from inner electrons and the nuclear Thomson amplitude.

- Our approximate treatment of partially filled shells is felt to be adequate for scattering from the ground states of atoms in most cases, but significant effects are expected for certain excited states (e.g., scattering from the excited 2p state of Hydrogen), or scattering at sufficiently low energies such that the scattering is dominated by loosely-bound electrons. A proper treatment (Carney et al., 2000b) includes contributions from incoherent elastic scattering and inelastic scattering from nearly degenerate subshells.

- We only consider scattering to lowest (2^{nd}) order in e^2. In some circumstances, such as the scattering from Helium (Lin et al., 1975), higher order contributions can be important.

As noted in the parenthetical thumbnail critique of each approximation in this list, the MFASF values hold special promise for accurate scattering predictions that go *beyond* that available from our current SM prescription. The major disappointment in our MFASF approach has been the inability to discover, to date, an angular dependence for the anomalous scattering factors that properly handle back angles of high energies for heavy atoms.

We strongly prefer the MFASF values over the RFASF values due to the fact that the modified relativistic form factors appear to correctly predict the forward-angle high-energy scattering limit. As a consequence, g ' (the real anomalous factor used with modified relativistic form factor, g) goes to zero at high energies. Under our assumption of angle-independent anomalous scattering factors, MFASF is a much better approximation than RFASF for non-forward angles for heavy atoms, especially at energies of 100 keV and above.[3] If a suitable angle dependence for the anomalous scattering factors could be devised, angle-*dependent* MFASF and angle-*dependent* RFASF could give similar predictions.

Table 2

Individual differential-scattering tables have been generated for a fixed Z and E on a 97-point grid for scattering angles 0-180º. The explicit angle grid is listed for reference in Table 2. The step size of the angle grid starts at 0.01º at forward angle and increases to 2.5º at back angles and is expected to easily support accurate interpolation to intermediate angles.

Table 3

Individual differential-scattering tables are computed for a single Z on a fixed 56-point grid for photon energies 0.05430-2754.1 keV, and stored as individual logical files (information blocks) within a UFO-structured library in a single file. The explicit energy grid for the tabulations is listed for reference in Table 3. For the most part, these energies have been selected for their experimental interest and are largely common x-ray and ã-ray energies. Because of the rapid variation in scattering as a function of energy, this energy grid is *NOT* expected to support accurate interpolation to intermediate energies. Some comments about interpolation of the SM results in energy are made subsequently.

In addition, for each of these approximations, two separate evaluations (stored in separate library files) are provided for the differential scattering cross sections; one file includes only the contribution from the Rayleigh (R) amplitude, and the second file includes the contribution of the summed Rayleigh and nuclear Thomson (R+NT) amplitudes. For example, the S-matrix differential cross sections for neutral Pb are stored in two separate files: '082_cs0sl_sm' includes only the contribution of Rayleigh (R) amplitudes; '082_cs0sl_sm+nt' contains the contribution of Rayleigh (R) and nuclear Thomson (NT) amplitudes.

Table 4

The value of the unpolarized differential scattering cross section for 59.54-keV photons scattered through 90º by Pb in various approximations is shown in Table 4. To increase one's confidence in utilization of these data files, prospective users are encouraged to find the corresponding values in the data files and compare them with the values listed in the table.

[3] Under the assumption of angle-independent anomalous scattering factors, f ' completely dominates f(q) in the real part of the scattering amplitude by 10° at about 1 MeV for Pb, while g' is still small compared with g(q) in the same circumstances. The SM/MFASF ratio for Pb of unpolarized differential cross sections varies in the range of about 0.8-1 for energies 0-100 keV, expanding to about 0.2-1 for energies 100-3000 keV. In contrast, the SM/RFASF ratio varies in the range of 1-10 for energies 0-100 keV, and 1-10^6 for energies 100-3000 keV.

7. Anomalous scattering factors (tables_ASF, data_ASF)

Anomalous scattering factors (ASF) prepared by previous authors has been restricted to keV energies (1-70 keV for Cromer and Liberman, 1-30 keV for Henke et al.), but our studies have required the values over a wider energy range. We have computed ASF values for all atoms over an expanded energy range of 0-10 MeV. These values are tabulated on a variable grid that allows accurate interpolation to intermediate energies. More details of our ASF calculation are provided in Kissel et al. (1995).

Two separate tabulations (stored in the folders 'tables_ASF' and 'data_ASF') of our anomalous scattering factors are provided, that differ in how the energy-dependent part of the bound-bound resonances are stored. The values in 'data_ASF' separately tabulate the real and imaginary anomalous scattering factors on independent grids. Further, only the constant contribution of bound-bound transitions is included in the real anomalous scattering factors; an analytic expression and separately tabulated bound-bound oscillator strengths are needed to compute the full result. As a consequence, these values can be accurately interpolated to all intermediate energies using appropriate algorithms, and can be safely used as input for further computations to the ASFTAB and FFTAB codes, as examples.

The tables in 'tables_ASF' explicitly include the full contribution of the bound-bound transitions and have been prepared by ASFTAB from data in 'data_ASF' folder. While these tables are more readily accessible for immediate use without further computations, they cannot be accurately interpolated to intermediate energies in all cases, as one cannot tabulate the full energy dependence of the bound-bound resonances on a dense enough grid.

In summary, the values in 'data_ASF' have been prepared for subsequent use in further calculations, while the values in 'tables_ASF' have been prepared for direct use without interpolation to intermediate energies.

A variety of notations, phase coventions and normalizations are in common use for anomalous scattering factors. We designate

(f ,f) as the Kissel and Pratt corrections for the relativistic form factor, f(q),
(g ,g) as the Kissel and Pratt corrections for the modified relativistic form factor, g(q),
(f CL, f CL) as the corrections defined by Cromer and Liberman (1970a,b),
(f1, f2) as the corrections defined by Henke et al (1981,1993),

to indicate the phase and magnitude of the anomalous scattering factors published by these authors. With this notation, we note the following relationships[4]

$$g(\omega) = f(\omega) - f(\infty),$$
$$g(\omega) = f(\omega),$$
$$f_{CL}(\omega) = f(\omega),$$
$$f_{CL}(\omega) = -f(\omega),$$
$$f1(\omega) = N + f(\omega),$$
$$f2(\omega) = f_{CL}(\omega) = -f(\omega).$$

Sample anomalous scattering factors extracted from the RTAB database are shown in Table 5.

An interesting feature of our ASF values that differs from other authors is the explicit inclusion of bound-bound resonant transitions. In our underlying model of single-electron transitions in a potential, a bound-bound resonant transition occurs at a single energy (our levels have no widths), the difference of the energies of the two orbitals involved in the transition. This infinitely narrow transition is manifested as a

[4] These equations are meant to indicate the phase and normalization relationships between the anomalous scattering factors of various authors. It would not be true, for example, that adding *N* to our value of f would yield exactly the f1 value as that published by Henke et al. (1993). Instead, adding *N* to our value of f would yield a quantity that could be compared directly to the f1 value published by Henke et al.

Table 5

delta-function spike in the imaginary scattering amplitude and a resonance approaching infinity in the real scattering amplitude. Although these explicit spikes and infinities are unphysical, the underlying strength of the transition is important and contributes significantly to the scattering at low energies. The inclusion of bound-bound transitions in our anomalous scattering factors is important for satisfying the Thomas-Reiche-Kuhn sum rule (see, Kissel et al., 1995), wherein an appropriate integral over all energies of the imaginary scattering amplitude should equal the number of electrons in the atom. In many cases, bound-bound transitions contribute 30% or more of the contribution to the TRK sum rule.

A challenge for evaluating anomalous scattering factors via the relativistic dispersion relation and the optical theorem involves energies above $2mc^2$. As discussed by Pratt et al. (1994), partitioning of the many particle scattering amplitude to yield R+NT+… introduces an additional contribution to the imaginary amplitude for Rayleigh scattering as computed by the optical theorem. Above $2mc^2$, to lowest order, one needs to subtract the contribution of bound-electron pair production[5] from that of photoeffect to correctly compute the total cross section. This insight settles a long standing quandary as it is known that the relativistic photoeffect cross section goes as *1/E* at high energies, and as a consequence, the dispersion integral is not convergent if photoeffect were the only contribution to lowest order at high energy. As with photoeffect, bound-electron pair production goes as *1/E* at high energies so the integration is naturally cut off at high energies. We utilize an estimate of the bound-electron pair production cross section for the non-relativistic K shell due to Costescu (see, for example, Bergstrom et al., 1997). In our evaluation of the anomalous scattering factors on 0-10 MeV, we carry out the integration for energies of 0-100 MeV.

The validity of this estimate for the total photon-atom cross section above $2mc^2$ has not been examined in detail. It is possible that this approximation in our evaluation of the anomalous scattering factors is responsible for the decreasing validity of our MFASF predictions at non-forward angles for energies above 100 keV.

Previous evaluations of anomalous scattering factors have ignored the issue of energies above $2mc^2$ by simply cutting off the integration at some suitably high energy. Besides being important for the evaluation of anomalous scattering factors in the 100-10,000 keV range, the behavior of the total cross section above $2mc^2$ effects values at lower energies by an overall constant. This is related to the high-energy limit corrections to the anomalous scattering factors of Cromer and Liberman prepared by Kissel and Pratt (1990).

All our anomalous scattering factors satisfy the TRK sum rule to a fraction of 1% (typically at the 0.01% level). The sum rule check is included as part of the output in the ASF files in 'data_ASF'. As an example, the TRK sum rule check in 'data_ASF/006_asf0sl' is

```
GPRIME: SUM-RULE CHECK ON CROSS SECTIONS;
     COMPUTED=   1.25405E+00 FROM BOUND-BOUND TRANSITIONS
                 4.74291E+00 FROM BOUND-FREE  TRANSITIONS
                 2.07488E-03 FROM HIGH-ENERGY LIMIT
                 5.99903E+00 TOTAL
    PREDICTED=   6.00000E+00
   DIFFERENCE=  -9.69774E-04  (-1.62E-02%)
```

The resonance structure from inclusion of bound-bound transitions is evident as the narrow peaks in the differential cross sections shown in Figure 1. For use in other contexts, it would likely be useful to convolve our values with a smoothing function of width 1-2 eV, especially for comparisons with predictions of other authors or with experiment in the resonance region.

[5] By bound-electron pair production, we mean pair production in which the electron of the pair is created is a bound state of the atom. Ordinarily, discussions of pair production involve the situation where both the electron and positron are created in the continuum.

8. Atomic form factors (data_MF, data_RF, data_NF)

We have independently evaluated the modified relativistic form factor (MF) and relativistic form factor (RF) even though these total-atom quantities have been previously published, for several reasons:

- we wanted all our data to be computed in exactly the same self consistent potential for detailed comparison with our S-matrix predictions;
- we required form factors that could be interpolated with very high accuracy to intermediate momentum transfers;
- in addition to total-atom values, we required systematic access to shell and subshell form factors to implement total-atom S-matrix cross sections.

Our total-atom and K-shell modified relativistic form factors are found to agree closely with the values published by Schaupp et al. (1983). Similarly, our total-atom relativistic form factors agree closely with the values published by Hubbell and Øverbø (1979).

Although the values are computed in a different atomic model, we have included the non-relativistic form factors (NF) of Hubbell et al. (1975) as a convenience to users of the RTAB database. The NF values are easily the approximation for elastic scattering in the widest use today. It will be natural in any investigation of scattering to relate more sophisticated predictions back to the non-relativistic form factors of Hubbell et al.

Table 6

In Table 6 we list selected form factors extracted from the RTAB database. Note that the MF and RF form factors are stored as form factor *per electron*, in contrast to the NF values. As a consequence, the MF and RF values in Table 6 have been multiplied by the appropriate number of electrons. An indication of the accuracy of our numerical evaluation of the form factor can be gleaned from the value of the total-atom RF in Table 6. As $f(0) \to N$, we see a relative error of less than about 1×10^{-8}.

We have observed that the MF values approach the same high-energy limit as our SM values within about the overall numerical accuracy of our calculations (see, for example, Kissel et al., 1995). Although not a proof, we suspect that the modified relativistic form factor essentially predicts the correct forward-angle high-energy limit of scattering, and we use MF as our practical evaluation of this limit. Due to this desirable feature of MF predictions, we tend to prefer MF to other form factors. It has also been our general experience, that the order of validity of form-factor-only predictions is MF, followed by NF, with RF yielding the poorest predictions.

9. Photoeffect cross sections, 0-50 MeV (data_PE)

Our evaluation of the real anomalous scattering factors proceeds from the relativistic dispersion relation, requiring an integral over all energies of the imaginary scattering amplitude. Using the optical theorem, we note that the photoeffect cross section dominates the imaginary scattering amplitude for x-ray and low-energy γ-ray energies.

Our evaluation of the photoeffect cross section starts with a modified version of the PIXS code due to Scofield (see, for example, Saloman et al., 1988). We directly compute subshell photoeffect cross sections in our potential to obtain total-atom cross sections up to several hundred keV. These values are stored in the RTAB database in files with the filename 'ZZZ_peIM', where 'ZZZ', 'I' and 'M' indicate the atomic number, ioniticity, and model as noted earlier, and '_pe' indicates that the file contains photoeffect cross sections. For example, the file 'data_PE/082_pe0sl' contains our direct evaluation of subshell and total-atom photoeffect cross sections from threshold to several hundred keV.

For higher energies, these values are smoothly joined to the total-atom values in the EPDL (Cullen et al., 1997) which extends the photoeffect cross sections up to 100 GeV. These extended photoeffect cross

sections are stored in a separate file. For example, the file 'data_PE/082_pe0slx' contains our *extended* total-atom photoeffect cross sections from threshold to 100 GeV.

Table 7

Selected total-atom photoeffect cross sections for Pb are listed in Table 7.

10. Bound-bound oscillator strengths (data_BBT, data_SRBBT)

Bound-bound oscillator strengths are needed in our evaluation of the anomalous scattering factors. As noted earlier, bound-bound transitions contribute as much as 30% or more to the Thomas-Reiche-Kuhn sum rule. Our evaluation of relativistic multipole bound-bound oscillator strengths follows the formulation of Scofield (1975).

The bound-bound oscillator strengths needed for our anomalous scattering factors connect occupied orbitals of the atom with unoccupied orbitals. These values are stored in the RTAB database in files with the filename 'ZZZ_bbtIM', where 'ZZZ', 'I' and 'M' indicate the atomic number, ioniticity, and model as noted earlier, and '_bbt' indicates that the file contains occupied-to-unoccupied bound-bound oscillator strengths. We consider all transitions down to 10^{-6} of the largest oscillator strength found. In order to satisfy this requirement, we often need to include transitions to states with principal quantum numbers up to 100 or more.

Table 8

For example, the file 'data_BBT/082_bbt0sl' contains our occupied-to-unoccupied bound-bound oscillator strenghts for Pb. Selected bound-bound oscillator strengths are listed in Table 8. The file contains a total of 1670 bound-bound transitions for a total oscillator strength of about 3.98; the maximum oscillator strength of about 1.06 is for the P1 P3 transition.

We also have need for oscillator strengths for transitions between occupied states of the atom. These transitions are needed to subtract *spurious resonances* from our S-matrix amplitudes. Recall that our SM prescription mixes predictions of S-matrix amplitudes for inner-shell electrons with modified relativistic form-factor predictions for outer-shell electrons. The S-matrix amplitudes, for a single electron transistion in a potential, include contributions for transitions to all bound and continuum states of the potential, including the occupied orbitals of the atom. If the total scattering amplitude for all occupied orbitals were computed solely via the S matrix, the contributions from transitions between occupied orbitals would vanish. If the transitions between occupied orbitals were not subtracted from the S-matrix amplitudes, however, spurious resonances connecting orbitals computed via the S matrix with orbitals computed via modified relativistic form factor would survive under our SM prescription. Consequently, we routinely subtract the contribution for spurious resonances (bound-bound transitions between occupied orbitals of the atom) from our S-matrix amplitudes.

Table 9

The spurious-resonance bound-bound oscillator strengths for transitions between occupied orbitals of the atom are stored in the RTAB database in files with the filename 'ZZZ_srbbtIM'. We consider all transitions that connect occupied orbitals of the atom, and sample values from 'data_SRBBT/082_srbbt0sl' are listed in Table 9. This file contains 276 transitions between the occupied orbitals of Pb, for a total oscillator strength of about 39.6; the maximum contribution is about 3.83 for the N5 N7 transition.

11. Selected source codes (code)

Source for several codes is being included in the RTAB database. These codes include:

- **RSCF** – our modified version of HEX (Liberman et al., 1971), a relativistic Dirac-Slater self consistent potential. These potentials are the basis of all of our further elastic scattering calculations. RSCF was used to produce the files in the 'data_SCF' folder of RTAB.
- **FORM** – our relativistic form-factor code. FORM easily computes subshell, shell and total-atom relativistic form factors and modified relativistic form factors, using the potential

supplied by RSCF. FORM was used to produce the files in the 'data_MF' and 'data_RF' folders of RTAB.

- **BBT** – our evaluation of relativistic multipole bound-bound oscillator strengths, using the potential supplied by RSCF. BBT was used to produce the files in the 'data_BBT' folder of RTAB.
- **GPRIME** – our relativistic anomalous scattering code. GPRIME requires input photoeffect cross sections, bound-bound oscillator strengths, and a potential. GPRIME generated the files in the 'data_ASF' folder of RTAB.
- **ASFTAB** – computes the energy-dependent part of the bound-bound contribution to the anomalous scattering factors, and reformats the files in 'data_ASF'. ASFTAB was used to prepare the files in the 'tables_ASF' folder of RTAB.
- **FFTAB** – computes elastic scattering cross sections based on the form-factor approximation, optionally including anomalous scattering factors. FFTAB can
  - utilize any of the form factors in 'data_MF', 'data_RF' or 'data_NF' (i.e., modified relativistic form factors, relativistic form factors, or non-relativistic form factors);
  - it can tabulate differential or integrated scattering cross sections;
  - it can evaluate unpolarized, linearly polarized (parallel or perpendicular), or circularly polarized (spin-flip or no-spin-flip) cross sections;
  - it can included anomalous scattering corrections, assuming angle independence or an angle dependence based on that of the non-relativistic Coulomb K shell (Bergstrom et al, 1997).
- **RAYLIB** – contains a collection of utility and support subprograms. RAYLIB contains all the support routines needed by the other codes listed here.

Each code is stored in a separate folder, and a Unix *make* file contains instructions for compilation and testing of the program. Each code has a test subdirectory containing input and output for the sample test cases.

Potential users may be particularly interested in the FFTAB code. As noted earlier, modified relativistic form factors with angle-independent anomalous scattering factors (MFASF) produce results close to those from our S-matrix prescription (SM) in many cases. MFASF cross sections at arbitrary photon energy, utilizing the data stored in the RTAB database, are easy to produce with FFTAB. This fact will be utilized for interpolation on SM values.

Another reason for potential interest in FFTAB is that it provides an avenue for easily going beyond the data stored in RTAB. Using these codes, it should be relatively easy to prepare cross sections for scattering from ions and excited atoms. With more effort it should be possible to utilize FFTAB to go beyond our SM predictions, incorporating experimental information (such as experimental binding energies) or atomic environment effects (as for scattering in plasmas or solids) in more realistic scattering calculations.

12. Selected work of other authors (others)

As a convenience to potential users, we have included selected work of other authors.

- **Cromer and Liberman** – the pioneering anomalous-scattering-factor code FPRIME and associated database due to Cromer and Liberman (1970a,b). We include a modified version of the 1983 code (Cromer, 1983) where we have included our high-energy-limit corrections (Kissel and Pratt, 1990).
- **Henke et al. (1993)** – 1-30 keV anomalous scattering factors based on experimental photoeffect cross sections.
- **Scofield (1973)** – a copy of the UCRL report with Dirac-Slater total-atom, shell and subshell photoeffect cross sections for Z=1-101, E=1-1500 keV.

13. Interpolating S-matrix cross sections

From Figure 1, it is evident that direct interpolation in energy on differential cross sections that include the contribution from bound-bound transitions can be problematic. Our experience suggests that the MFASF approximation should serve as a reasonable basis for smoothing the SM values, and that heavy atoms at high energy and back angles are the most challenging cases to consider.

Table 10

In Table 10 we list the ratio of SM/MFASF unpolarized differential scattering cross sections for selected energies and angles for Pb. We display only selected energies, but all energies on our 56-point grid have been checked and the values in Table 10 are representative of the behavior of the SM/MFASF ratio. (A similar table for the SM/RFASF ratio would show variations of a factor of 10^6.) We observe that the SM/MFASF ratio is reasonably smooth at all energies and angles, and the ratio is very close to one for the bulk of the anomalous scattering region for L-shell and lower energies (<~20 keV for Pb). While the SM/MFASF ratio varies by a factor of about 5 as shown in Table 10, the underlying differential cross sections differ by a factor of 10^7.

Focusing on 90° scattering for Pb, we have interpolated the SM/MFASF ratio using 2-point linear interpolation from the nearest-neighbor grid points of our 56-point energy grid, neglecting the point under consideration. That is, for example, to test the accuracy of interpolating from our 56-point grid at 59.54 keV, we have interpolated the value of the SM/MFASF ratio at 59.54 keV using the ratio values at 57.53 and 66.83 keV. Our assumption is that this will provide a pessimistic estimate of the error for interpolating intermediate ratios as we have purposely ignored data in the table and there are significantly better interpolation methods that could be employed. We find that error in the interpolated ratio is accurate to much less than 1% for energies below the K-shell binding energy (about 88 keV for Pb), and generally about 1% or less at higher energies. The exceptions are 2% errors for 80-90 keV, 3% errors around 250 keV and 1173 keV, and a 9% error at 1408 keV.

We expect generally then, that our energy grid is sufficient to interpolate SM unpolarized differential scattering cross sections by interpolating on the SM/MFASF ratio to an accuracy of about 2% or better for energies less than about 1 MeV for all angles for all atoms. An estimate of the SM value at an intermediate energy can be obtained by scaling the MFASF predictions of FFTAB by the interpolated SM/MFASF ratio. Further efforts to confirmation these expectations should be undertaken in the future.

14. Conclusions

A substantial body of data has been generated in support of elastic photon-atom scattering investigations of Kissel, Pratt and co-workers. These data are being provided in a format that should allow immediate use for further scattering studies and other research. The methods described here for neutral atoms have direct extension to ions and excited atoms, and should serve as a basis for studies of scattering from atoms in environments such as plasmas and solids.

Acknowledgements

The work described in this report is the direct result of a 25-year collaboration with Richard Pratt who suggested this subject as the author's thesis subject and who has mentored the author's efforts since then. Early progress on development of the S-matrix approach was aided by H. K. Tseng and Walter Johnson. Mihai Gavrila and Viroica Florescu have provided many important insights and stimulating discussions on scattering theory. Much of this work was stimulated by the involved interest of experimentalists such as Martin Schumacher, Prabhakar Kane, David Bradley and Odair Gonçalves. Specific help with the generation of photoeffect cross sections and bound-bound oscillator strengths was provided by James Scofield. Further encouragement and understanding has resulted from stimulating interactions with Suprakash Roy, Swapan Sen Gupta, Paul Bergstrom, Jr., Adrian Costescu, David Shaffer, Bin Zhou,

Tihomir Suric, David Templeton, John Hubbell and others. This work has been supported in part by Lawrence Livermore National Laboratory under the auspices of the U.S. Department of Energy under contract number W-7405-Eng48.

References

Basavaraju G., Kane P. P., Sahasha M. L., Kissel L. and Pratt R.H. (1995) Elastic scattering of 88.03 keV gamma rays – revisited, *Phys. Rev. A* **51**, 2608-10.

Brown G. E., Peierls R. E. and Woodward J. B. (1955) The coherent scattering of ã-rays by K electrons in heavy atoms. I. Method, *Proc. R. Soc. (London)* **A227**, 51-8.

Bergstrom, Jr., P. M., Kissel L., Pratt R. H. and Costescu A. (1997) Investigation of the angle dependence of the photon-atom anomalous scattering factors, *Acta Cryst.* **A 53**, 7-14.

Carney J. P. J. and Pratt R. H. (2000) Constructing adequate predictions for photon-atom scattering: A composite approach, submitted to *Phys. Rev. A* (University of Pittsburgh Report Pitt-515).

Carney J. P. J., Pratt R. H., Kissel L., Roy S. C. and Sen Gupta S. K. (2000a) Rayleigh scattering from excited states of atoms and ions, submitted to *Phys. Rev. A* (University of Pittsburgh Report Pitt-509).

Carney J. P. J., Pratt R. H., Manakov N. L. and Meremianin A. V. (2000b) Dependence of photon-atom scattering on energy resolution and target angular momentum, accepted for *Phys. Rev. A* (University of Pittsburgh Report Pitt-512).

Creagh D. C. and McAuley W. J. (1992) X-ray dispersion corrections, in *International Tables for Crystallography*, Vol. C, edited by A. J. C. Wilson, Kluwer Academic Publishers, Dordrecht, pp. 206-22.

Cromer D. T. (1974) Dispersion effects, in *International Tables for X-ray Crystallography*, Vol. IV, edited by J. A. Ibers and W. C. Hamilton, Kynoch Press, Birmingham (present distributor Kluwer Academic Publishers, Dordrecht) pp. 148-50.

Cromer D. T. (1983) Calculation of anomalous scattering factors at arbitrary wavelengths, *J. Appl. Cryst.* **16**, 437-437.

Cromer D. T. and Liberman D. A. (1970a) Relativistic calculation of anomalous scattering factors for x-rays, Los Alamos Scientific Laboratory Report LA-4403, Los Alamos, New Mexico, pp.163.

Cromer D. T. and Liberman D. A. (1970b) Relativistic calculation of anomalous scattering factors for x rays, *J. Phys. Chem.* **53**, 1891-8.

Cromer D. T. and Liberman D. A. (1976) Anomalous scattering factors for Co $Ká_1$ radiation, *Acta Cryst.* A**32**, 339-40.

Cromer D. T. and Liberman D. A. (1981) Anomalous dispersion calculations near to and on the long-wavelength side of an absorption edge, *Acta Cryst.* A**37**, 267-68.

Cullen D. E., Hubbell J. H. and Kissel L. (1997) EPDL97: The evaluated photon data library, Lawrence Livermore National Laboratory report UCRL-50400, vol. 6, rev. 5, available from the National Technical Information Service, U.S. Department of Commerce, 5285 Port Royal Road, Springfield, VA 22161.

Gonçalves O., Cusatis C. and Mazzaro I. (1993) Solid-state effects on Rayleigh scattering experiments - Limits for the free atom approximation, *Phys. Rev. A* **48**, 4405-10.

Gonçalves O., Santos W. M., Eichler J. and Borges A. M. (1994) Rayleigh scattering from crystals and amorphous structures, *Phys. Rev. A* **49**, 889-93.

Henke B., Gulliksen E. M. and Davis J. C. (1993) X-Ray interactions – photoabsorption, scattering, transmission, and reflection at E=50-30,000 eV, Z=1-92, *At. Data Nucl. Data Tables* **54**, 181-342; erratum **54**, 349-349.

Henke B., Lee P., Tanaka T. J., Shimabukuro R. L. and Fujikawa B. K. (1981) The atomic scattering factor, f1 + if2, for 94 elements and for the 100 to 2000 eV photon energy region, in *Low Energy X-ray Diagnostics – 1981 (Monterey), AIP Conf. Proc. No. 75*, edited by D. T. Attwood and B. L. Henke, American Institute of Physics, New York, pp. 340-88.

Hubbell J. H. and Øverbø I. (1979) Relativistic atomic form factors and photon coherent scattering cross sections, *J. Phys. Chem. Ref. Data* **8**, 69-105.

Hubbell J. H., Veigele W. J., Briggs E. A., Brown R. T., Cromer D. T. and Howerton R. J. (1975) Atomic form factors, incoherent scattering functions, and photon scattering cross sections, *J. Phys. Chem. Ref. Data* **4**, 471-538; erratum (1977) **6**, 615-16.

Jung M., Dunford R. W., Gemmell D. S., Kanter E. P., Krassig B., LeBrun T. W., Southworth S. H., Young L., Carney J. P. J., LaJohn L., Pratt R. H. and Bergstrom Jr., P. M. (1998) Manifestations of non-local exchange, electron correlation and dynamic effects in X-ray scattering, *Phys. Rev. Lett.* **81**, 1596-1599.

Johnson W. R. and Cheng K. T. (1976) Elastic scattering of 0.1-1-MeV photons, *Phys. Rev. A* **13**, 692-8.

Johnson W. R. and Feiock F. D. (1968) Rayleigh scattering and the electromagnetic susceeptibility of atoms, *Phys Rev.* **168**, 22-31.

Kane P.P., Kissel L., Pratt R. H. and Roy S. C. (1986) Elastic scattering of -rays and x-rays by atoms, *Phys. Rep*. **140**, 75-159.

Kissel L., Biggs F. and Marking T. R. (1991a) UFO (UnFold Operator) user guide: part 1 - overview and brief command descriptions, Sandia National Laboratories report SAND82-0396, 97 pp., available from the National Technical Information Service, U.S. Department of Commerce, 5285 Port Royal Road, Springfield, VA 22161.

Kissel L., Marking T. R. and Biggs F. (1991b) UFO (UnFold Operator) - default data format, Sandia National Laboratories report SAND91-0490, 28 pp., available from the National Technical Information Service, U.S. Department of Commerce, 5285 Port Royal Road, Springfield, VA 22161.

Kissel L. and Pratt R. H. (1990) Corrections to tabulated anomalous scattering factors, *Acta Cryst.* **A46**, 170-5.

Kissel L. and Pratt R. H. (1985) Rayleigh scattering: elastic photon scattering by bound electrons, in *Atomic Inner-Shell Physics*, edited by B. Crasemann, Plenum Press, New York, pp. 465-532.

Kissel L., Zhou B., Roy S. C., Sen Gupta S. K. and Pratt R. H. (1995) Validity of form-factor, modified-form-factor, and anomalous-scattering-factor approximations in elastic scattering calculations, *Acta Cryst.* A**51**, 271-88.

Liberman D. A., Cromer D. T. and Waber J. T. (1971) Relativistic self-consistent field program for atoms and ions, *Comput. Phys. Commun.* **2**, 107-13.

Liberman D. A. and Zangwill A. (1984) A relativistic program for optical response in atoms using a time-dependent local density approximation, *Comput. Phys. Commun*. **32**, 75-82.

Lin C-P; Cheng K-T and Johnson, W.R. (1975) Rayleigh scattering of photons by helium, *Phys. Rev. A* 11, 1946-56.

Pratt R. H., Kissel L. and Bergstrom, Jr., P. M. (1994) New relativistic S-matrix results for scattering - beyond the usual anomalous factors/beyond impulse approximation, in *X Ray Resonance (Anomalous) Scattering*, G. Materlik and C. Sparks, eds., Elsevier, Amsterdam, pp. 9-33.

Saloman E. B., Hubbell J. H. and Scofield J. H. (1988) X-ray attenuation cross sections for energies 100 eV to 100 keV and elements Z = 1 to Z= 92, *At. Data Nucl. Data Tables* **38**, 1-197.

Schaupp D., Schumacher M., Smend F., Rullhusen P. and Hubbell J. H. (1983) Small-angle Rayleigh scattering of photons at high energies: Tabulations of relativistic HFS modified atomic form factors, *J. Phys. Chem. Ref. Data* **12**, 467-512.

Scofield J. H. (1973) Theoretical Photoionization Cross Sections from 1 to 1500 keV, unpublished Lawrence Livermore Laboratory Report UCRL-51326, Livermore, California.

Scofield J. H. (1975) Radiative transitions, in Atomic Inner-Shell Processes, edited by B. Crasemann, Academic Press, New York, pp. 265-292.

Table 1. Contents of the RTAB database (version 2.0).

Folder name	Description of contents
tables_SM	Differential scattering tables via numerical S-matrix approximation (SM) due to Kissel and Pratt
tables_MFASF	Differential scattering tables via modified relativistic form factor (MF) with angle-independent anomalous scattering factors (ASF)
tables_RFASF	Differential scattering tables via relativistic form factor (RF) with angle-independent anomalous scattering factors (ASF)
tables_MF	Differential scattering tables via modified relativistic form factor (MF)
tables_RF	Differential scattering tables via relativistic form factor (RF)
tables_NF	Differential scattering tables via non-relativistic form factors (NF) due to Hubbell et al. (1975) ***not in DS potential***
tables_ASF	Tables of relativistic anomalous scattering factors. Differs from 'data_ASF' in that energy-dependent part of the bound-bound transitions has been incorporated in the tables, but result is not reliable for accurate interpolation near resonances.
data_SCF	Dirac-Slater (DS) potentials
data_ASF	Relativistic anomalous scattering factors. Differs from 'tables_ASF' in that energy-dependent part of the bound-bound resonances is not directly included in table (bound-bound oscillator strengths stored separately), allowing accurate interpolation to intermediate energies
data_MF	Tables of total-atom, shell and subshell modified relativistic form factors (MF)
data_RF	Tables of total-atom and shell relativistic form factors (RF)
data_NF	Tables of total-atom non-relativistic form factors (NF) due to Hubbell et al. (1975) ***not in DS potential***
data_PE	Photoeffect cross sections
data_BBT	Bound-bound oscillator strengths (occupied-unoccupied)
data_SRBBT	Spurious-resonance bound-bound oscillator strengths (occupied-occupied)
others	Scattering work of other authors: Cromer and Liberman (1983) – FPRIME code, ***not in DS potential*** Henke et al. (1993) – f1,f2 anomalous factors, ***not in DS potential*** Scofield (1973) – photoeffect cross sections 1-1500 keV
codes	Source for selected codes useful for the evaluation of elastic scattering amplitudes

Table 2. Explicit values (in degrees) for 97-point angle grid for differential cross-section tabulations.

Scattering angle grid, è (degrees)				
0	3.5	40.0	90.0	140.0
0.01	4.0	42.5	92.5	142.5
0.02	5.0	45.0	95.0	145.0
0.04	6.0	47.5	97.5	147.5
0.06	7.0	50.0	100.0	150.0
0.1	7.5	52.5	102.5	152.5
0.2	8.0	55.0	105.0	155.0
0.3	9.0	57.5	107.5	157.5
0.4	10.0	60.0	110.0	160.0
0.5	12.5	62.5	112.5	162.5
0.6	15.0	65.0	115.0	165.0
0.7	17.5	67.5	117.5	167.5
0.8	20.0	70.0	120.0	170.0
1.0	22.5	72.5	122.5	172.5
1.2	25.0	75.0	125.0	175.0
1.5	27.5	77.5	127.5	177.5
1.7	30.0	80.0	130.0	180.0
2.0	32.5	82.5	132.5	
2.5	35.0	85.0	135.0	
3.0	37.5	87.5	137.5	

Table 3. Explicit values (in keV) for 56-point photon-energy grid for differential-cross section tabulations.

Photon energy grid, E (keV)		
0.05430	22.16	411.8
0.1085	27.47	444.0
0.1833	36.03	468.1
0.2770	46.00	511.0
0.3924	57.53	661.6
0.5249	59.54	723.3
0.6768	66.83	779.1
0.8486	77.11	867.5
1.041	83.78	889.2
1.254	90.88	964.2
1.486	98.44	1004.8
2.622	111.3	1086.0
4.086	121.8	1112.2
5.415	122.9	1173.2
6.404	145.4	1274.5
8.048	244.5	1332.5
11.22	279.2	1408.1
14.41	344.2	2754.1
17.48	411.1	

Table 4. Values of the unpolarized differential elastic-scattering cross section for 59.54-keV photons scattered through 90° by Lead (Pb, Z=82) in various approximations, as stored in the specified data files of the Rayleigh scattering database.

filename	Rayleigh amplitude approximated by	Includes nuclear Thomson amplitudes?	dó/dÙ (barns/sr)
tables_SM/082_cs0sl_sm	SM	No	2.35580E+00
tables_SM/082_cs0sl_sm+nt	SM	Yes	2.36658E+00
tables_MFASF/082_cs0sl_mfasf	MFASF	No	2.50924E+00
tables_RFASF/082_cs0sl_rfasf	RFASF	No	2.33913E+00
tables_MR/082_cs0sl_mf	MF	No	2.68907E+00
tables_RF/082_cs0sl_rf	RF	No	3.17852E+00
tables_NF/082_cs0h75_nf	NF	No	2.56186E+00

Table 5. Values of the anomalous scattering factors for selected atoms at 8.04778 keV from the RTAB database.

atom	Filename	f = f'$_{CL}$	g = f - f (¥)	f1 = N + f	f = g = -f$_{CL}$ = -f2
C (Z=6)	tables_ASF/006_asftab0sl	1.91297E-02	2.12046E-02	6.01913E+00	-9.55063E-03
Ne (Z=10)	tables_ASF/010_asftab0sl	1.04035E-01	1.11061E-01	1.01040E+01	-8.57632E-02
Al (Z=13)	tables_ASF/013_asftab0sl	2.16604E-01	2.29718E-01	1.32166E+01	-2.50211E-01
Zn (Z=30)	tables_ASF/030_asftab0sl	-1.55537E+00	-1.46193E+00	2.84446E+01	-6.94718E-01
Sn (Z=50)	tables_ASF/050_asftab0sl	3.73172E-02	3.46528E-01	5.00373E+01	-5.50974E+00
Pb (Z=82)	tables_ASF/082_asftab0sl	-4.08364E+00	-3.08775E+00	7.79164E+01	-8.68796E+00

Table 6. Selected zero-momentum-transfer (x = 0 $Å^{-1}$) form-factor values for Pb from the RTAB database.

case	N, Number of electrons	Type of form factor	Value of form factor [6]	Filename
Total atom	82	MF	8.1004097E+01	tables_MF/082_mf0sl|m=TOTAL|t=82*y
		RF	8.1999995E+01	tables_RF/082_rf0sl|m=TOTAL|t=82*y
		NF	8.20000E+01	tables_NF/082_nf0h75
K shell	2	MF	1.7225122E+01	tables_MF/082_mf0sl|m=K|t=2*y
L shell	8	MF	7.6671533E+01	tables_MF/082_mf0sl|m=L|t=8*y
M shell	18	MF	1.7754837E+01	tables_MF/082_mf0sl|m=M|t=18*y
N shell	32	MF	3.1876648E+01	tables_MF/082_mf0sl|m=N|t=32*y
O shell	18	MF	1.7983587E+01	tables_MF/082_mf0sl|m=O|t=18*y
P shell	4	MF	3.9993610E+00	tables_MF/082_mf0sl|m=P|t=4*y
L1 shell	2	MF	1.9210517E+00	tables_MF/082_mf0sl|m=L1|t=2*y
L2 shell	2	MF	1.8988850E+00	tables_MF/082_mf0sl|m=L2|t=2*y
L3 shell	4	MF	3.8472164E+00	tables_MF/082_mf0sl|m=L3|t=4*y

[6] The MF and RF values are stored as form factor per electron in the RTAB database. *N*, the number of electrons, has multiplied the MF and RF values listed here.

Table 7. Selected total-atom photoeffect cross sections for Pb are extracted from the file 'data_PE/082_pe0slx' in the RTAB database.

Photon energy (keV)	**σ_{PE} (barns/atom)**
5.28789E-03	2.92837E+07
1.00000E-02	1.45907E+07
1.00000E-01	4.50548E+06
1.00000E+00	1.78931E+06
1.00000E+01	4.31911E+04
1.00000E+02	1.80601E+03
1.00000E+03	6.22580E+00
1.00000E+04	1.79000E-01
1.00000E+05	1.46000E-02
1.00000E+06	1.42800E-03
1.00000E+07	1.42500E-04
1.00000E+08	1.42400E-05

Table 8. Selected occupied-to-unoccupied bound-bound oscillator strengths for Pb are extracted from the file ‘data_BBT/082_bbt0sl’ in the RTAB database.

Transition		**Transition energy (keV)**	**Initial state, occupied (n_1, $\hat{e}_1$)**	**Final state, unoccupied (n_2, $\hat{e}_2$)**	**Ä = $_{2-1}$**	**f_{total} (per initial electron)**	**$f_{electric}$ (per initial electron & final hole)**	**$f_{magnetic}$ (per initial electron & final hole)**
K	Q1	8.83511E+01	(1,-1)	(7,-1)	0	3.55161E-08	0.00E+00	1.78E-08
K	P3	8.83486E+01	(1,-1)	(6,-2)	1	1.08147E-04	4.06E-05	1.89E-09
K	P2	8.83469E+01	(1,-1)	(6, 1)	1	6.95786E-05	5.22E-05	0.00E+00
K	P5	8.83524E+01	(1,-1)	(6,-3)	2	7.32820E-08	1.22E-08	1.88E-12
L3	Q1	1.30365E+01	(2,-2)	(7,-1)	-1	2.71613E-05	1.36E-05	7.60E-12
P1	P3	9.80446E-03	(6,-1)	(6,-2)	1	1.06036E+00	3.98E-01	3.19E-17

Table 9. Selected spurious-resonance bound-bound oscillator strengths for Pb are extracted from the file 'data_SRBBT/082_srbbt0sl' in the RTAB database.

Transition		**Transition energy (keV)**	**Initial state, occupied (n_1, $\hat{e}_1$)**	**Final state, occupied (n_2, $\hat{e}_2$)**	**Ä = $_{2-1}$**	**f_{total} (per initial electron)**	**$f_{electric}$ (per initial electron & final hole)**	**$f_{magnetic}$ (per initial electron & final hole)**
K	L1	7.24965E+01	(1,–1)	(2,-1)	0	3.68471E-04	0.00E+00	1.84E-04
K	L2	7.31016E+01	(1,–1)	(2, 1)	1	2.16403E-01	1.08E-01	0.00E+00
K	L3	7.53146E+01	(1,–1)	(2,–2)	1	3.48130E-01	8.70E-02	3.71E-06
L1	L2	6.05025E-01	(2,-1)	(2, 1)	1	3.25986E-02	1.63E-02	0.00E+00
L3	M5	1.05507E+01	(2,–2)	(3,-3)	1	1.81068E+00	3.02E-01	5.31E-08
M1	N7	3.67986E+00	(3,-1)	(4,-4)	3	1.12378E-05	1.40E-06	1.37E-14
N5	N7	2.64735E-01	(4,-3)	(4,-4)	1	3.82834E+00	4.79E-01	9.97E-13

Table 10. SM/MFASF ratio of unpolarized differential scattering cross sections at selected energies and angles for Pb. While the SM/MFASF ratio varies by about a factor of 5 in this table, the underlying differential cross sections vary by a factor of 10^7.

Photon energy (keV)	$d\sigma^{SM}/d\sigma^{MFASF}$					
	0°	**10°**	**30°**	**60°**	**90°**	**120°**
0.0543	1.000	1.000	1.000	1.000	1.000	1.000
0.1833	1.000	1.001	1.001	1.000	1.001	1.001
0.3924	1.000	1.000	1.000	1.000	1.001	1.000
1.041	1.000	1.000	1.000	0.999	0.998	0.998
5.415	1.000	1.000	0.999	0.996	0.994	0.992
8.048	1.000	1.000	0.999	0.994	0.992	0.989
17.48	1.000	1.000	0.997	0.989	0.983	0.975
22.16	1.000	1.000	0.996	0.984	0.975	0.965
59.54	1.000	0.999	0.991	0.958	0.939	0.916
145.4	1.000	0.998	0.978	0.901	0.872	0.823
279.2	0.999	0.996	0.947	0.770	0.728	0.730
411.8	0.999	0.994	0.919	0.696	0.744	0.783
779.1	0.998	0.985	0.817	0.628	0.703	0.643
889.2	0.998	0.982	0.805	0.588	0.636	0.539
1173.2	0.999	0.975	0.787	0.453	0.412	0.313
1332.5	0.999	0.966	0.759	0.369	0.325	0.252
2754.1	0.999	0.895	0.429	0.238	0.295	0.278

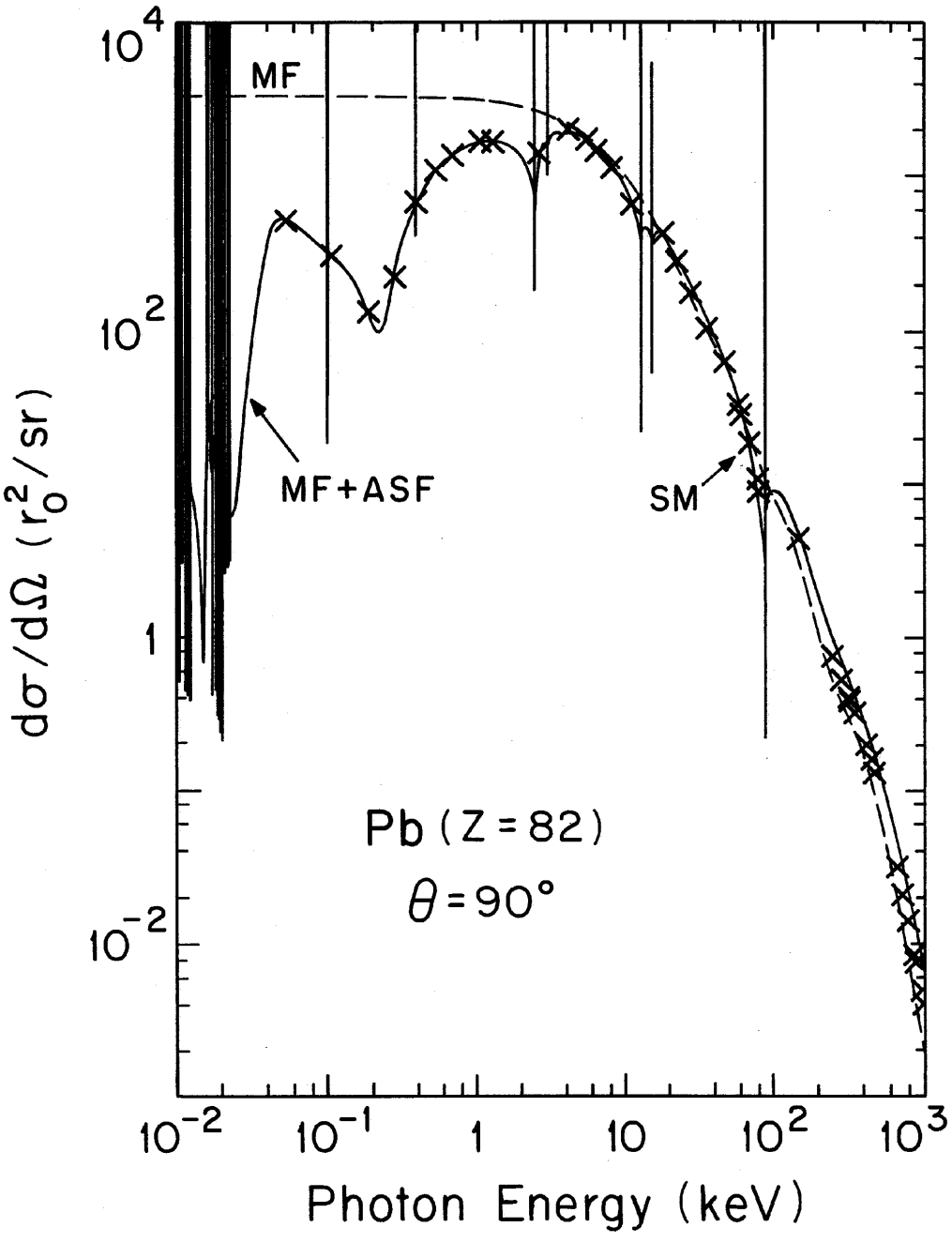

Figure 1. The resonant structure of elastic scattering through 90° for Lead (Pb, Z=82), observed in our SM and ASF calculations, is usually ignored in simpler approximations.